

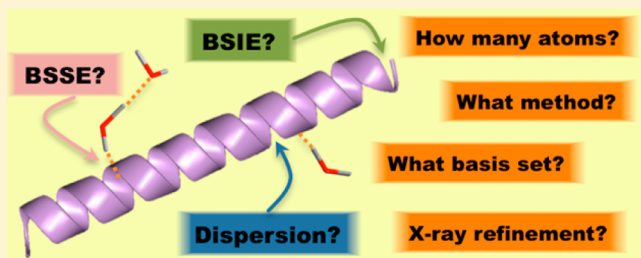
Efficient Methods for the Quantum Chemical Treatment of Protein Structures: The Effects of London-Dispersion and Basis-Set Incompleteness on Peptide and Water-Cluster Geometries

Lars Goerigk and Jeffrey R. Reimers*

School of Chemistry, The University of Sydney, New South Wales 2006, Australia

S Supporting Information

ABSTRACT: We demonstrate how quantum chemical Hartree–Fock (HF) or density functional theory (DFT) optimizations with small basis sets of peptide and water cluster structures are decisively improved if London-dispersion effects, the basis-set-superposition error (BSSE), and other basis-set incompleteness errors are addressed. We concentrate on three empirical corrections to these problems advanced by Grimme and co-workers that lead to computational strategies that are both accurate and efficient. Our analysis encompasses a reoptimized version of Hobza’s P26 set of tripeptide structures, a new test set of conformers of cysteine dimers, and isomers of the water hexamer. These systems reflect features commonly found in protein crystal structures. In all cases, we recommend Grimme’s DFT-D3 correction for London-dispersion. We recommend usage of large basis sets such as cc-pVTZ whenever possible to reduce any BSSE effects and, if this is not possible, to use Grimme’s gCP correction to account for BSSE when small basis sets are used. We demonstrate that S–S and C–S bond lengths are very prone to basis-set incompleteness and that polarization functions should always be used on S atoms. At the double- ζ level, the PW6B95-D3-gCP DFT method combined with the SVP and 6-31G* basis sets yields accurate results. Alternatively, the HF-D3-gCP/SV method is recommended, with inclusion of polarization functions for S atoms only. Minimal basis sets offer an intriguing route to highly efficient calculations, but due to significant basis-set incompleteness effects, calculated bond lengths are seriously overestimated, making applications to large proteins very difficult, but we show that Grimme’s newest HF-3c correction overcomes this problem and so makes this computational strategy very attractive. Our results provide a useful guideline for future applications to the optimization, quantum refinement, and dynamics of large proteins.



1. INTRODUCTION

Computational studies of proteins range in nature from methods that seek to avoid structural details, such as bioinformatics,¹ to methods based on qualitative structure–activity relationships (QSAR)² to methods based on empirical molecular-mechanics (MM) force fields³ to methods involving partial quantum-mechanical (QM) treatments (QM/MM)⁴ to methods based solely on quantum descriptions of the electronic motions.^{5–7} QM/MM or QM treatments in this context are often restricted to Hartree–Fock (HF) or density functional theory (DFT⁸) because of computational limitations.⁴ Full QM treatments of big systems are usually carried out by various linear-scaling fragmentation schemes or by using computationally fast levels of theory in combination with high parallelization on CPU or GPU high-performance clusters.^{5–7,9} The advantage of incorporating the quantum mechanical electronic structure of proteins is that such QM calculations are less biased toward the features used in the parametrization of empirical methods. This, in principle, allows treating a broader range of systems, including those that contain new or unusual structural features.

QM and QM/MM treatments of proteins are often carried out using Hartree–Fock (HF) or DFT approximations combined with small basis sets such as double- ζ or even

minimal basis sets.^{4,7} When doing this, one faces three problems: a proper treatment of London-dispersion (attractive van-der-Waals forces), the intramolecular basis-set-superposition error, and other errors due to the incompleteness of small basis sets. Even extensive calculations, such as the PW91/6-31(+)-G* optimization of the 150 000 atom photosystem-I trimer using linear-scaling DFT, suffer from these problems.⁵ It is well-known that HF and DFT do not correctly describe London-dispersion effects,¹⁰ which, however, are crucial to the structural stability of biomolecular systems.¹¹ Nevertheless, many studies, for example, in the field of quantum refinement of protein X-ray crystal structures, have been reported for HF or DFT approximations without taking these effects into account.⁴ For smaller to medium-sized systems, and later also for larger van-der-Waals and protein–ligand complexes, it has been demonstrated that dispersion-corrected density functional theory is an accurate remedy to overcome the London-dispersion problem of DFT.¹² Various methods for treating dispersion effects with DFT have been devised.¹³ Herein, we concentrate on Grimme’s widely used and established DFT-D3

Received: April 18, 2013

approach,¹⁴ which has been shown to work excellently for noncovalent interaction energies,^{14,15} general thermochemistry,¹⁶ and geometries,^{14b,17,18} without any significant additional cost. We demonstrated that DFT-D3 also improves the structural features of the lysozyme protein in the framework of a quantum refinement scheme that we are currently developing.⁶ This study also showed that dispersion-corrected corrected HF theory (HF-D3) is a valuable tool, which is in accordance with other findings for noncovalent interaction energies and geometries.^{7,14b,16,19}

However, previous studies on proteins (including ours) have neglected important errors induced by using small basis sets. We follow here a classification allowing these errors to be described as two separate problems: the basis-set-superposition error (BSSE) and the basis-set-incompleteness error (BSIE).^{20,21} BSSE describes the well-known fact that noncovalent interaction energies are overestimated when using incomplete, atom-centered, one-particle basis sets. In the picture of a noncovalently bound dimer, one can imagine that the monomers “borrow” atomic basis functions from each other, when calculating the absolute energy of the dimer. Compared to a treatment of each isolated monomer, the dimer itself is therefore artificially overstabilized. This problem affects, of course, not only energies but also all properties derived from them such as geometries. For the intermolecular case of a noncovalently bound dimer, the counterpoise correction of Boys and Bernadi is a useful remedy.²² Although questioned frequently,²³ it has become a popular, albeit cost-expensive, tool to estimate BSSE effects. Note that other corrections have been proposed, each with their own advantages and disadvantages.²⁴

In the same spirit as for the dimer case, one can also imagine that parts of a single molecule borrow basis functions from other regions of the same system. This has been defined as intramolecular BSSE (IBSSE). In our context, it is important to note that IBSSE has been found to influence the conformational energy profile of peptides owing to the important role of inter-residue interactions,²⁵ and therefore, it is expected that it will also significantly affect protein structures. It is rather difficult to apply these above-mentioned BSSE corrections to IBSSE, as they could possibly introduce covalent-bond breakage, unusual spin states, or unchemical fragments. They can also introduce arbitrariness that makes them technically and conceptually very difficult to apply in a “black-box” generalized fashion. Finally, these corrections are also time-consuming, prohibiting their application to large systems. Kruse and Grimme have addressed these shortcomings with their newly developed gCP approach (geometrical counterpoise correction).²¹ The name stems from the fact that gCP is only based on the atomic coordinates of the system and does not directly take into account the atomic basis functions, making it very time-efficient. In principle, gCP shares some parallels to the DFT-D3 correction. It is an additive atomic pairwise correction that is evaluated at basically no computational cost when combined with a HF or DFT calculation. It contains three empirical parameters fitted to Boys–Bernardi counterpoise corrections for a set of intermolecular interaction energies. However, it is straightforward to apply this method also for the treatment of IBSSE. Currently, gCP is available for four small basis sets, including one minimal basis set, and it has been designed for the treatment of large systems. In their original work, Kruse and Grimme demonstrated its applicability to various test cases, including a minimal-basis-set optimization of the crambine protein comprising about 600 atoms.

In a separate study, Kruse et al. enhanced the popular B3LYP/6-31G* model chemistry with the help of DFT-D3 and gCP.²⁶ It has been often argued²⁶ that this level of theory relies for its widespread success on error compensation between missing London-dispersion and overstabilization by BSSE. However, this error compensation is completely unforeseeable, and Kruse et al. demonstrated that actually B3LYP-D3-gCP/6-31G* is a more reliable method than the original, providing improved accuracy for general thermochemistry and, in particular, for organic reaction energies and barrier heights. Herein, we will elaborate whether unforeseeable error-compensation effects are also observed in geometry optimizations and whether a combination of D3 and gCP also provides higher robustness in these situations.

The gCP approach effectively corrects for BSSE but does not include BSIE effects. Sure and Grimme outlined how HF, even when corrected with D3 and gCP, significantly overestimates the lengths of polar bonds when applied with a minimal basis set.²⁷ However, HF with the above-mentioned corrections is a valuable tool for the treatment of large systems, and they addressed this BSIE problem by introducing a third, empirical correction. It was fitted against hybrid-DFT bond-lengths obtained with a triple- ζ basis for organic molecules. The entire approach was dubbed HF-3c, as it contains the three corrections for dispersion, BSSE, and BSIE. Applications to noncovalently bound dimers, large van-der-Waals complexes, and gas-phase structures of small proteins showed that indeed HF-3c is a promising, time-efficient new tool that is worthwhile to investigate further.

As mentioned before, we have engaged in developing a full quantum refinement scheme for protein X-ray structures.⁶ In this framework, we are faced with all three problems addressed above, as the usage of high-level QM methods, which describe London-dispersion effects, or large basis sets is prohibited. Particularly, the BSSE and BSIE problems have not been addressed thoroughly in this context. Previous studies ignored these effects, partially because of the lack of efficient corrections and partially also because error compensation was expected.⁴ However, we argue that having a more reliable method should always be favored over unforeseeable error-compensation effects and we address this issue herein. In this study, we concentrate on the effects of method, London-dispersion, BSSE, and BSIE. Before thoroughly investigating their effects on protein crystal structures, their influence on peptide model systems must first be established. Quantum chemical studies of peptides in the gas-phase provide first insights into method performance and help in the development of low-level methods for larger proteins.

Most previous model studies of calculating protein properties have concentrated on relative conformational energies of either amino acids,²⁸ or di- and tripeptides,²⁹ or also some biologically relevant tetrapeptides.^{11b,30} To enable focus on the quality of optimized geometries in a systematic fashion, Hobza and co-workers introduced a test set of 26 tripeptide structures under the name P26.³¹ The tripeptides in this set contain aromatic side chains and are therefore ideal test cases to study London-dispersion and IBSSE. Initially, Hobza and co-workers briefly considered the effects of London-dispersion using Grimme's older DFT-D2^{12d} correction, but errors induced by small basis sets were not considered.

We also introduce a new test set for method quality based on the conformers of cysteine dimers linked through a disulfide bridge. In our previous QM refinement study, we identified the

description of cysteines as crucial to obtain proper agreement with measured X-ray reflections.⁶ Particularly, disulfide bridges were shown to be very sensitive to the method of choice, and our new test set reveals difficult cases.

When treating protein crystal structures, one also has to deal with enclosed clusters of water molecules. Any theoretical method that works well for proteins must inherently also describe water clusters properly. This has rarely been regarded in this context, and therefore, we examine the influence of BSSE and BSIE on the structures of water hexamers.³²

The test sets are briefly introduced in the next section. Section 3 describes all relevant theoretical and computational details. Section 4 addresses the tests sets under consideration of the outlined problems. We are confident that this study sheds light into the various effects of chosen method and small basis sets and that our findings can be used as a guideline for method development for large proteins.

2. TEST SETS

2.1. P26 Set. Hobza's P26 set³¹ comprises a total of 26 conformers of 5 peptides that contain aromatic side chains. Table 1 shows each peptide's composition and number of

Table 1. Composition of Hobza's P26 Benchmark Set for Peptide Geometries³¹

acronym	sequence	no. conformers
FGG	phenylalanyl-glycyl-glycine	7
GFA	glycyl-phenylalanyl-alanine	4
GGF	glycyl-glycyl-phenylalanine	4
WG	tryptophyl-glycine	5
WGG	tryptophyl-glycyl-glycine	6

conformers. The conformations were selected from a total of 76 structures and encompass a diversity of backbone and side chain arrangements. Detailed information about the generation of the conformers is given in ref 31.

The P26 structures were obtained by MP2/cc-pVTZ³³ optimization. While this level of theory is not sufficient to describe accurately the relative conformational energies of peptides,^{16,31} Hobza et al. have argued that for covalent bonds it is qualitatively acceptable. However, some of the P26 conformers also contain hydrogen bonds, and it has been shown for tetrapeptides that IBSSE produces a sizable overestimation of hydrogen-bond strength at the MP2/cc-pVTZ level.³⁰ Also it is known that diffuse functions improve the description of hydrogen bonds,³⁴ and the most straightforward way in which these structures could be improved would be to use aug-cc-pVTZ³³ instead of cc-pVTZ. However, such an expansion also introduces costly diffuse functions with high angular momenta that are actually not needed for the description of hydrogen bonds, with previous benchmark calculations on water clusters showing that it is sufficient to just use one set of diffuse s- and p-functions on each heavy atom.^{16,35} We follow this strategy and dub this modified basis set aug*-cc-pVTZ.

We reoptimised the P26 data set at the MP2/aug*-cc-pVTZ level, and all structures are provided in the Supporting Information (SI). Comparisons with the original structures show that covalent bond lengths are basically not affected while hydrogen bonds increase on average by 0.04 Å. Root-mean-square-deviations (RMSD) between the original and reoptimised structures are usually below 0.05 Å (see Table S1 in the

SI). Only in two cases the deviations are larger: for GGF05 the RMSD is 0.510 Å and for WG10 it is 0.116 Å. The average RMSD for the entire set is 0.046 Å. While this difference is small compared to the gross effects that we focus on, having the most reliable reference data is always an advantage.

Finally, we would like to comment on the accuracy of the structures. The MP2 structures should not be understood as a quantitative reference. There is still a portion of remaining IBSSE (between 5 and 10% for the chosen basis set), not all of the electron correlation is covered, and MP2 itself has inherent problems with London-dispersion. However, the purpose of this study is to examine lower levels of theory and to demonstrate the effects of London-dispersion, BSSE, and BSIE. The MP2 structures are only used to qualitatively support our conclusions and findings. We additionally carried out analyses with SCS-MP2³⁶/cc-pVTZ and B2PLYP-D3³⁷/cc-pVTZ structures, and the main conclusions for the lower levels of theory are still the same (see the SI). However, a thorough discussion of these additional structures is beyond the point of this manuscript.

2.2. CYS2 Set. In our previous quantum refinement study, we found that it is particularly difficult to describe disulfide bridges appropriately and that statistical analysis tools such as *R*-factors³⁸ are very sensitive to errors made for cysteine residues.⁶ Relative conformational energies of cysteine monomers in the gas-phase have been investigated thoroughly in quantum chemical benchmark studies,^{16,28c} but no analogous test set is available for disulfide-linked cysteines. We introduce the model system shown in Figure 1, in which methylamide and

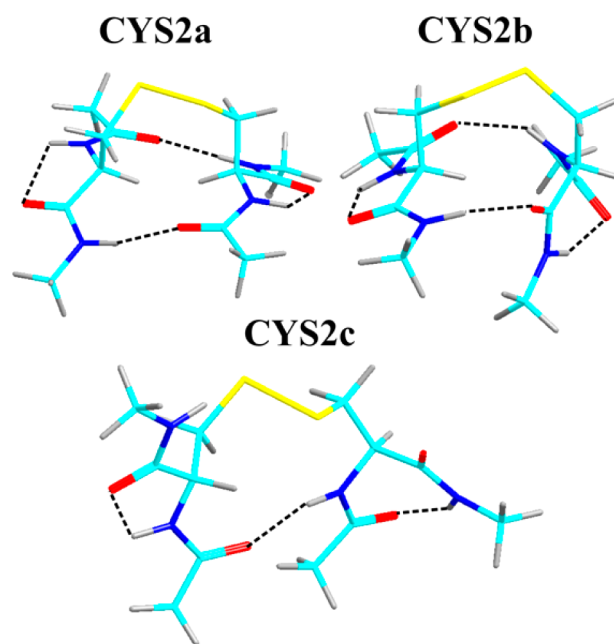


Figure 1. Three conformers of the cysteine-dimer model. Hydrogen bonds are marked with dashed lines.

acetyl groups cap the C- and N-termini of the cysteine backbones, respectively, to mimic effects of a continuing peptide backbone. In fact, although this system is considered to be a model in our context, it also has been studied experimentally in the past, with a focus on reactivity with oxygen and on electronic circular dichroism spectroscopy.³⁹

We carried out a thorough conformational analysis of the system and will elaborate these results elsewhere. For this

study, we picked the three conformers shown in Figure 1, named CYS2a–CYS2c, on the basis of their structural appearance, and optimized them at the MP2/aug*-cc-pVTZ level of theory, to be consistent with our treatment of P26 (Cartesian coordinates of all structures are provided in the SI). CYS2a and CYS2b appear more rigid due to two hydrogen bonds connecting the adjacent backbones with each other. CYS2c only has one hydrogen bond connecting the two backbones and has overall a less rigid appearance.

2.3. Water Hexamer Test Set. The structures of the *cage*, *prism*, and *book* isomers of water hexamers have been resolved by broadband rotational spectroscopy.³² The authors provided accurate experimental estimates and vibrationally averaged MP2 results for the O–O distances in those clusters. These structures have been used by Hujo and Grimme for an evaluation of van-der-Waals (DFT-NL) functionals for large basis sets that do not suffer from BSSE.¹⁸ Their analysis showed that using the experimentally obtained structures gives an almost quantitative picture of the tested QM methods, even though they were not vibrationally averaged. We will follow the same procedure here in this work, with a focus on smaller basis sets, BSSE and BSIE.

3. TECHNICAL DETAILS

All calculations were carried out with TURBOMOLE 6.4.⁴⁰ The convergence criterion for each SCF step was set to $10^{-7} E_h$. Geometries were optimized until the energy change between two subsequent optimization steps was below the same energy threshold as for the SCF calculations. MP2 optimizations of the structures of the P26 and CYS2 sets were carried out using aug*-cc-pVTZ, as defined in Section 2. All MP2 calculations were sped up with the resolution-of-the-identity (RI) approximation, and respective auxiliary basis functions were taken from the TURBOMOLE library.⁴¹ Subsequent optimizations of all systems were carried out by Hartree–Fock (HF) and the following DFT methods: BLYP,^{42,43} BP86,^{42,44} PBE,⁴⁵ B97-D,^{12d} TPSS,⁴⁶ B3LYP,⁴⁷ PBE0,⁴⁸ PW6B95,⁴⁹ and BHLYP.⁵⁰ These calculations were carried out with the cc-pVTZ triple- ζ basis set,³³ Pople's 6-31G*⁵¹ and Ahlrichs' SVP and SV⁵² double- ζ sets, and Huzinaga's minimal basis set MINIS,⁵³ which was taken from the EMSL basis-set exchange library.⁵⁴ Except for MINIS, the calculation of Coulomb contributions of HF and the DFT methods was carried out with the RI-J approximation, with auxiliary basis sets again being taken from the TURBOMOLE library.⁵⁵ All DFT calculations were carried out with the TURBOMOLE grid *mS*;⁵⁶ test calculations using the TURBOMOLE "reference" grid, a grid comparable to Gaussian's ultrafine grid, indicated the quality of this approach.

The HF and DFT calculations were additionally carried out with Grimme's D3 and/or gCP corrections. These are independent additive corrections of the form:

$$E^{\text{HF/DFT-D3-gCP}} = E^{\text{HF/DFT}} + E^{\text{D3}} + E^{\text{gCP}} \quad (1)$$

where $E^{\text{HF/DFT}}$ is the original HF or DFT energy, E^{D3} is the DFT-D3/HF-D3 energy contribution, and E^{gCP} is the gCP energy contribution.

The D3 method is well established.¹⁴ It is an additive, atomic pairwise correction that considers the correct asymptotic R^{-6} long-range and the R^{-8} medium-range behaviors for interatomic distances. Herein, we applied the D3-correction with the Becke–Johnson damping function that adds a constant contribution even at the unified-atom limit.^{14b} This correction

is sometimes called DFT-D3(BJ)/HF-D3(BJ) to distinguish it from the first D3 version.^{6,14b,15,16} However, DFT-D3(BJ) has been shown to be superior to the previous version and has been recommended as a standard procedure for dispersion-corrected DFT and HF,^{14b} and hence, we skip the suffix in the parentheses. The D3-correction depends on three empirical parameters that have been optimized for HF and about 50 DFT methods and implemented in Grimme's DFT-D3 program⁵⁷ as well as in, e.g., TURBOMOLE 6.4.

The gCP correction accounts for BSSE without any significant cost, making it particularly relevant for applications to large systems.²¹ It contains three empirical parameters that have been fitted to Boys–Bernardi counterpoise corrections to intermolecular interaction energies for the basis sets 6-31G*, SVP, SV, and MINIS. Different sets of parameters were proposed for HF and for DFT. Unlike DFT-D3, there are no functional-specific parameters and all parameters are the same for all DFT approximations. The benefit of combining DFT-D3 and gCP has been demonstrated.^{21,26} We use Grimme's freely available program gCP.⁵⁷

Sure and Grimme developed a correction for basis-set incompleteness, which addresses the problem of elongated bond lengths for HF combined with minimal basis sets.²⁷ This correction depends on three additional empirical parameters fitted using a set of B3LYP triple- ζ structures of organic molecules. The correction is specifically designed for a basis set, called MINIX, which is a mixture of MINIS, additionally augmented with one set of p-type polarization functions for certain elements. Elements beyond potassium are described by a double- ζ basis, but this is of no concern in our present context because the heaviest element studied is sulfur. This new correction is combined with D3 and gCP, and the entire approach is called HF-3c ("3 corrections"). These corrections were obtained with a special program obtained from the authors.

4. RESULTS AND DISCUSSION

First, we focus our discussion on London-dispersion and IBSSE, demonstrating problems that arise owing to basis-set incompleteness. The HF-3c method is then applied to remedy these problems.

4.1. Discussion of the P26 Set. 4.1.1. Effects of the D3-Correction on the cc-pVTZ Level. It has already been outlined that it is crucial to use dispersion-corrections in DFT optimizations of biologically relevant structures. For instance, in their original study of P26, Hobza et al. recommended TPSS-D/6-311++G(3df,3pd) as a promising DFT method.³¹ However, this recommendation was based on a variant^{34b} of the older DFT-D2 correction.^{12d} Additionally, those TPSS-D results were compared with B3LYP/6-31G* calculations and, as expected, that latter level of theory underperforms because of the lack of a dispersion correction. Dispersion-corrected B3LYP was not discussed at all, nor was pure B3LYP treated with the same basis set as TPSS-D.

Therefore, we start the discussion of the P26 set with a short analysis of London-dispersion effects based on DFT-D3 using the same basis set for each method. In this section, we restrict our discussion to the cc-pVTZ basis set and the TPSS, B3LYP, PW6B95, and HF methods. The analysis is based on root-mean-square deviations (RMSDs) involving the Cartesian coordinates of all atoms, and they can be influenced by both short-range effects in covalent bonds and long-range inter-residue effects influenced by London-dispersion and hydrogen

bonding. A detailed list of all RMSDs of these tested methods with respect to MP2/aug*-cc-pVTZ geometries for all 26 structures is given in the SI in Table S3. As can be seen therein, for all DFT methods, the effect of the dispersion correction is large and using DFT-D3 reduces the RMSDs significantly, for example, by up to 1 Å in the case of conformer FGG252. The only exception is structure FGG215 for the TPSS and B3LYP functionals. During both optimizations (with and without D3-correction), the phenyl-ring turned away from the terminating glycyl part leading to very similar RMSDs around 0.66 Å. PW6B95-D3 does not show this behavior. Table 2 shows

Table 2. Averaged RMSDs for All Atoms (Å) for P26 with Respect to MP2/aug*-cc-pVTZ Geometries^a

	uncorrected	with D3
TPSS	0.671	0.141
B3LYP	0.684	0.120
PW6B95	0.496	0.111
HF	0.630	0.115

^aRMSDs are shown for TPSS, B3LYP, PW6B95 and HF at the cc-pVTZ level with and without dispersion-corrections.

RMSDs averaged over all 26 systems. The averaged RMSD of 0.671 Å for TPSS is reduced to 0.141 Å for TPSS-D3, which is a bit better than the value of 0.151 Å for TPSS-D2 and the previously reported value of 0.16 Å for TPSS-D2 based on MP2/cc-pVTZ structures. B3LYP-D3 has a slightly lower averaged RMSD of 0.120 Å, and PW6B95-D3 gives the lowest value with 0.111 Å.

Using the D3-correction has a large effect on HF optimized structures and improves them in all cases, including FGG215 (Table S3, SI). The final averaged RMSD of 0.115 Å is better than that for B3LYP-D3 and compares well with that obtained using PW6B95-D3 (Table 2).

4.1.2. Effects of gCP on the 6-31G* Level. Next, we address the effect of BSSE on peptide structures for small basis sets. We first discuss People's 6-31G* set, as it is very widely used. Figure 2 shows averaged RMSDs for P26 using the same four methods as discussed in the previous section as well as the BP86 functional. BP86/6-31G* without any corrections has

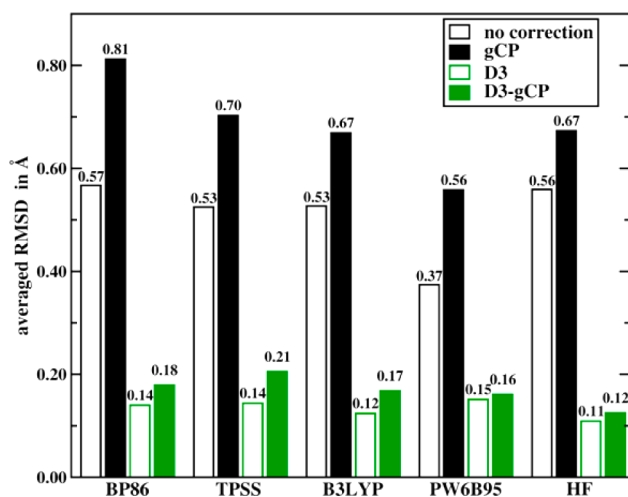


Figure 2. RMSDs for all atoms (Å) averaged over the P26 set for five different methods with and without DFT-D3 and gCP corrections. The 6-31G* basis set was used in all cases.

been proposed as a reliable method for efficient peptide and protein optimization.^{4a,c} If none of the corrections are applied, then the RMSDs of these five methods are between 0.53 Å and 0.57 Å, with BP86/6-31G* having the highest value, and PW6B95 being an exception with 0.37 Å. When the structures are optimized using the gCP correction, all RMSDs increase. The smallest increase is observed for HF; however, it is still sizable with an RMSD of 0.67 Å for HF-gCP compared to 0.56 Å for HF. The effects of BSSE for B3LYP are similar to those for HF but much larger for the remaining three methods. Particularly, BP86 shows the largest effect with an increase from 0.57 Å to 0.81 Å. These numbers reflect what has already been described for intermolecular BSSE: the overstabilization leads to shorter distances between the aromatic moieties and the opposite termini of the peptide backbones. Having shown that these systems are strongly influenced by BSSE, the lower RMSDs for uncorrected methods on their own imply that BSSE corrections should not be used. We further comment on this later, after having discussed the effects of the simultaneous application of both corrections.

As Figure 2 shows, adding just a dispersion correction to the pure QM method improves the RMSDs to between 0.11 Å and 0.15 Å. However, there is still a stabilizing contribution from BSSE, and for DFT-D3-gCP and HF-D3-gCP, we still observe a slight increase compared to DFT-D3 and HF-D3. When both corrections are applied, the lowest RMSD is observed for HF-D3-gCP (0.125 Å), followed by PW6B95-D3 (0.161 Å), B3LYP-D3-gCP (0.168 Å), BP86-D3-gCP (0.179 Å), and TPSS-D3-gCP (0.205 Å). These numbers clearly show that the popular BP86/6-31G* and B3LYP/6-31G* combinations should not only be used with caution for energetic properties (as shown for B3LYP²⁶) but also for geometries. The effects of BSSE and dispersion are also depicted for BP86 and the FGG99 conformer in Figure 3.

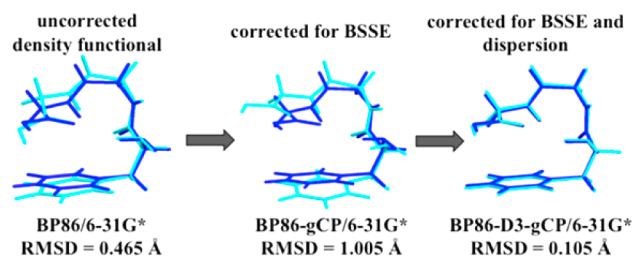


Figure 3. BP86/6-31G* (light blue) structures of the FGG99 conformer compared with the MP2 geometry (dark blue). The effects of adding the DFT-D3 and gCP corrections are shown. RMSDs with respect to MP2 are also shown.

One argument against using gCP would be the lower RMSDs calculated for the respective methods without this correction, relying on error compensation effects to provide better results. However, it has been outlined for B3LYP/6-31G* applied to thermochemical problems²⁶ that error-compensation effects are not always foreseeable. Herein, we observe the same for geometries, for instance, for the WG10 and WGG05 conformers. In both cases, B3LYP yields a higher RMSD than B3LYP-gCP, which is contrary to the averaged RMSDs of the whole set (see the SI). Also, an increase in the RMSD when adding the gCP correction simply means that the results are still influenced by BSSE, and for the sake of getting the right result for the right reason, we argue that it is better to have a

more robust approach, even though it might lead to an increase in statistical errors for some properties.

We draw the same conclusion when looking at this issue from a slightly different point of view. Inspection of Figure 2 reveals that the differences in RMSDs between results for the pure and the gCP-corrected methods are larger than between DFT-D3/HF-D3 and DFT-D3-gCP/HF-D3-gCP. However, these absolute differences vary in terms of the underlying functional, which makes it very difficult to completely explain this behavior. We are dealing here with the interplay of three different aspects (the functional, D3, and gCP) that in combination yield different potential energy surfaces with different global minima. This observation stresses again that the various effects influencing these energy surfaces are unforeseeable and that, in terms of robustness and consistency, it is safer to apply all corrections. In accordance with our findings and the above-mentioned previous findings for thermochemistry, we recommend to use both the D3- and gCP corrections for geometries to get a better picture of the “true” performance of a method. Only this allows us to evaluate and compare various DFT and HF approaches on an equal footing, as done in the following section.

So far we have concentrated mainly on how London-dispersion and BSSE effects influence the distances between the aromatic moieties and the adjacent peptide backbones. However, also hydrogen bonds are present in some systems, and analysis of their influence gives us further insight into the feasibility of using small basis sets for peptide optimizations. Figure 4 shows the hydrogen-bond lengths averaged over all

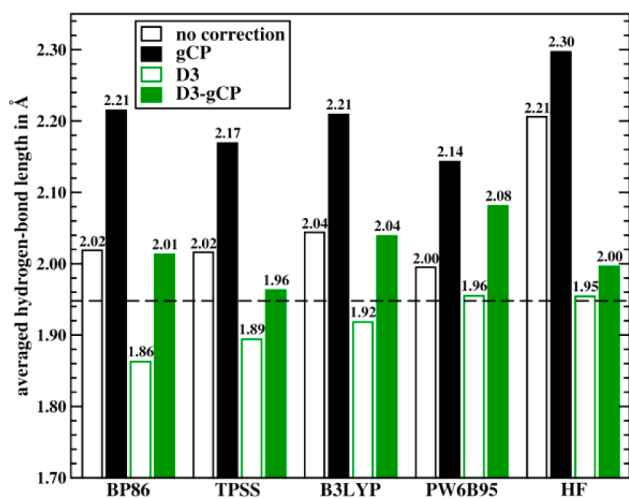


Figure 4. Averaged hydrogen-bond lengths, in Å, for the P26 set for five different methods with and without DFT-D3 and gCP corrections. The 6-31G* basis set was used in all cases. The dashed line shows the averaged value for MP2/aug*-cc-pVTZ as a qualitative guideline.

systems for the same five methods as discussed before. Overall, the same trends are observed as for the RMSDs: whenever the gCP correction is applied, the hydrogen-bond lengths increase by up to 0.2 Å for the DFT methods. Only HF seems to be less affected by BSSE with changes of less than 0.1 Å. Interestingly, the averaged hydrogen-bond lengths are the same for BP86 and BP86-D3-gCP. This is also seen for B3LYP, perhaps indicating why these uncorrected methods are widely used and provide good results. This error cancellation is not observed for the other three methods. Particularly HF needs the DFT-D3 correction to shorten the bond-lengths. Thus, we have

demonstrated that there is a sizable influence of BSSE on the hydrogen-bond lengths and the distances between the two adjacent parts of the peptides. Next, we will discuss the influence of basis sets.

4.1.3. RMSDs for Various Basis Sets and Methods. We have now established that a combination of the two corrections is beneficial for both DFT and HF leading to a more robust treatment with less unforeseeable error-compensation effects. Finally, we compare various density functionals and HF with each other and discuss basis-set effects. Figure 5 shows averaged

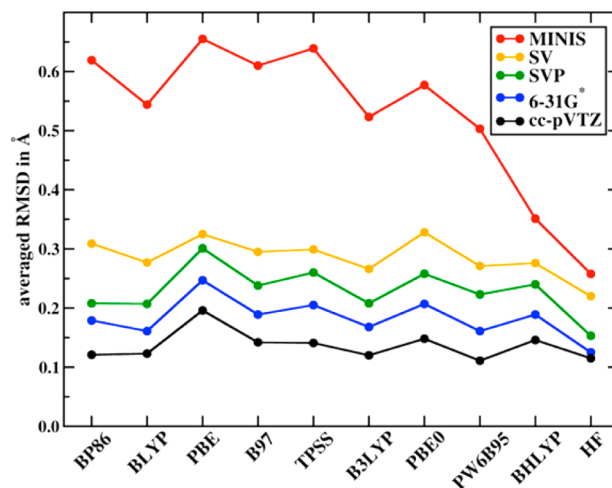


Figure 5. RMSDs for all atoms (Å) averaged over the P26 set for DFT-D3-gCP methods and HF-D3-gCP for five different basis sets.

RMSDs for P26 for cc-pVTZ and the four basis sets for which the gCP correction was parametrized; full details are provided in the SI in Table S3. For cc-pVTZ, dispersion-corrected GGA functionals BP86-D3 and BLYP-D3 yield slightly lower RMSDs (about 0.12 Å) than TPSS-D3 and B97-D3 (0.14 Å), competing with hybrid functionals. PBE-D3 yields the worst RMSD at the cc-pVTZ level of almost 0.2 Å. The best result of this study is found for PW6B95-D3 (0.111 Å), which is in accordance with previous findings for this functional in terms of robustness for accurate energetic and geometries.^{14b,16} B3LYP-D3 follows closely, whereas PBE0-D3 and BHLYP-D3 behave similarly to GGA functionals. HF-D3 is competitive with PW6B95-D3 with an RMSD of 0.115 Å.

For small basis sets, the gCP correction is important. However, gCP does not correct for BSIE, and the RMSDs for all DFT methods shown in Figure 5 for 6-31G* are slightly higher than those for cc-pVTZ. Also, the differences between the various functionals are now larger. The best two DFT methods are BLYP-D3-gCP and PW6B95-D3-gCP with RMSDs of 0.161 Å. The basis set dependence of HF is much less than that of DFT, which is why HF-D3-gCP/6-31G* has an RMSD of 0.125 Å, very close to that of HF-D3/cc-pVTZ. When going to the Ahlrichs basis sets SVP and SV, the RMSDs increase again for all methods with SV having significantly higher RMSDs. The lack of polarization functions in SV is a likely reason for this. The trends for all methods remain basically the same and HF-D3-gCP yields in all cases the lowest RMSDs (0.153 Å for SVP and 0.220 Å for SV).

The RMSDs for the MINIS minimal basis set are disproportionately large. For the DFT methods, MINIS gives different trends to those found for the other basis sets (Figure 5). Most DFT methods lead to RMSDs in a range between 0.48

Å and 0.64 Å, with BHLYP being the exception with an RMSD of 0.351 Å, which is clearly contrary to the trends found for larger basis sets. HF-D3-gCP is the only method that does not show such a big increase. In fact, its RMSD of 0.256 Å is similar to or better than the RMSDs for the DFT-D3-gCP/SV methods. We analyzed the results further and could conclude that even for those smaller basis sets, the same basic trends in terms of BSSE and dispersion are observed as discussed for 6-31G*, which means that neither of the corrections is responsible for these high increases in the RMSDs. In fact, this only leaves one likely explanation, the basis-set incompleteness itself.

Based solely on RMSDs, we can recommend the BLYP-D3, PW6B95-D3, and HF-D3 methods, in combination with gCP for small basis sets. However, the effects of BSIE are analyzed in the next section, and it is addressed whether these recommendations are also valid for a reliable description of covalent bond lengths.

4.1.4. Understanding the BSIE Effects on Covalent Bonds.

The analysis of RMSDs for P26 demonstrated the benefits of including dispersion and BSSE corrections in DFT and HF optimizations. We have also mentioned that adding these corrections influences hydrogen-bond lengths and distances between aromatic moieties and the adjacent backbone termini. However, when using very small basis sets, the RMSDs increase noticeably, and one possibility for this is the BSIE. An ideal method for applications such as quantum refinement of protein X-ray structures must also yield adequate bond lengths, as these do contribute to the *R*-factors that compare theoretical models with measured X-ray reflections.

We analyze four types of bonds: the carbonyl bond, the C–N peptide bond, the C–C_α bond, and the N–C_α bond. We note in passing that adding both corrections to DFT does not have a sizable effect on covalent bond lengths and has only a marginal effect for HF, slightly shortening the bonds (see Table S6, SI, for more for information). Therefore, our analysis includes those corrections in the following. The results for the five GGA and meta-GGA functionals are averaged as well as the calculated bond lengths for the four hybrid functionals. Additionally, the results for HF-D3(-gCP) are discussed. These results are shown for all basis sets and the four different types of bonds in Figure 6. For all bond lengths and all methods, we see the same basis-set dependence. The less complete the basis set, the longer the bond lengths get. Whereas 6-31G* and SVP results are still similar to those for cc-pVTZ, stripping the basis set of polarization functions (SV basis set) leads to elongation, particularly for the polar carbonyl group. The next largest elongation is seen when going from the SV to the minimal basis set. For QM refinement purposes, the bonds for MINIS are unacceptably long. Note, that this is not only true for HF but for DFT as well.

Using big basis sets is prohibited when treating big biomolecules and a compromise has to be found between computational time and basis-set incompleteness. For this purpose, the averaged calculated bond lengths for the MP2 structures are shown as guidelines in Figure 6. It is textbook knowledge that HF theory yields too short bond lengths,⁵⁸ which can be seen for the cc-pVTZ, 6-31G*, and SVP results. Due to basis-set incompleteness, HF-D3-gCP/SV, however, agrees very well with the MP2 results. For (meta-)GGA DFT, it is known that bond lengths are slightly too long,⁵⁸ which is also observed herein, in particular for the SV and MINIS basis sets. Hybrid DFT results lie in between GGA and HF as they

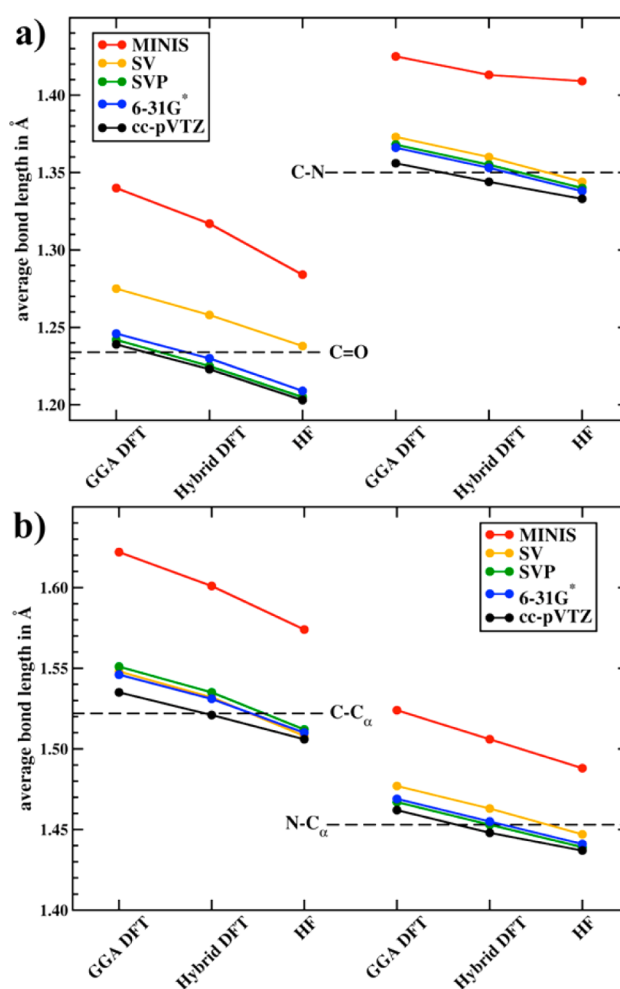


Figure 6. Averaged bond-lengths for four different types of bonds (Å). (a) Carbonyl and peptide bonds; (b) lengths between C_α and the carbonyl C-atoms or the peptide N-atoms. The values are averaged over all (meta-)GGA or hybrid DFT methods. Also, values for HF are shown. Five different basis sets are discussed. The dashed lines show the average bond-lengths for MP2/aug*-cc-pVTZ.

contain portions of both methods. Also, here, cc-pVTZ and the double- ζ sets with polarization functions can be recommended.

We therefore extend our recommendations from the previous section by saying that, based on the findings for P26, a hybrid functional such as PW6B95-D3 empirically gives the best results when used with cc-pVTZ, or with gCP and 6-31G* or SVP. When computational restrictions limit the basis-set size to at most SV, we recommend using the HF-D3-gCP method instead.

4.2. Results for the CYS2 Set. **4.2.1. Discussion of RMSDs.** RMSDs for the three CYS2 conformers (see Figure 1 and Section 2.2) are calculated without taking into account the terminating methyl groups, as they are rather floppy and rotation of these might affect the RMSDs and hence lead to artifacts in their interpretation. These RMSDs for all tested levels of theory are listed in the SI, and we only restrict ourselves to a very short description of these, as the overall trends are similar to those observed for the P26 set.

The trends for the RMSDs of the CYS2a and CYSb conformers are very similar to each other (Table S8, SI) as a result of the rigidity induced by the two hydrogen bonds connecting the adjacent backbones with each other (see Figure

1), while for the more flexible CYS2c conformer a larger range of the RMSDs is observed. Applying the gCP correction leads to structures with slightly higher RMSDs, which means again that BSSE-uncorrected methods overestimate the noncovalent interactions; however, also, exceptions are seen: for instance, HF-D3-gCP/6-31G* yields a lower RMSD than HF-D3 for CYS2a (0.046 Å vs 0.067 Å, see Table S8, SI), which again underlines our argumentation that it is safer to apply both corrections to avoid unforeseeable error-compensation effects. The basis set dependence of averaged RMSDs is also very similar to that of P26 (see Figure S1, SI). Smaller basis sets yield higher RMSDs, and in general, the same methods as for P26 can be recommended. An important difference between the P26 and the CYS2 sets is discussed in the next section.

4.2.2. BSIE Effects on S–S and C–S Bonds. The basis set and method dependence of bond lengths involving carbon, oxygen, and nitrogen is the same as discussed for P26. Figure 7,

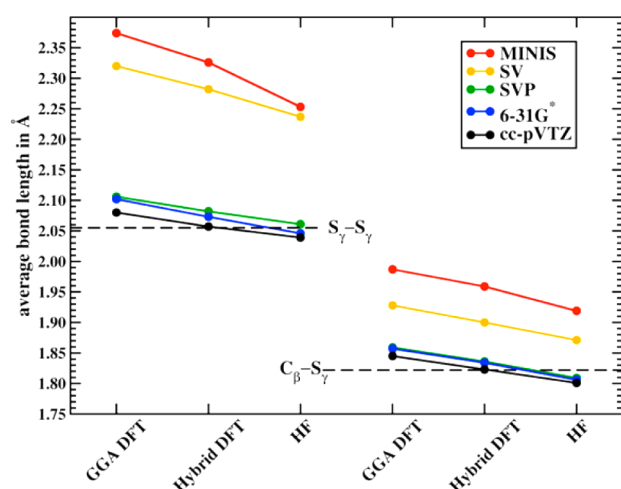


Figure 7. Averaged bond lengths for the disulfide bridge and the C–S bonds in the cysteine dimers (Å). The values are averaged over all (meta)-GGA or hybrid DFT methods. Also, values for HF are shown. Five different basis sets are discussed. The dashed lines show the average bond-lengths for MP2/aug*-cc-pVTZ.

therefore, only shows S_γ – S_γ and C_β – S_γ bond lengths averaged over the three conformers, for the (meta)-GGAs, the hybrid functionals, and HF. In principle, it is again observed that bond lengths get shorter when increasing the amount of Fock exchange. Hybrid functionals give very similar results to MP2 using cc-pVTZ but again the smaller 6-31G* and SVP empirically give better values for HF. The necessity for polarization functions is enhanced for S–S and C–S bonds compared to the bonds discussed for P26. Indeed, the SV basis set is no longer useful for S–S and C–S bonds, with the averaged S–S bond lengths ranging between 2.24 Å and 2.32 Å, compared to 2.06 Å for MP2 or the crystallographic value of around 2.02–2.03 Å.⁵⁹ Note, however, that the effect is also seen for the C_β – S_γ bond, but that it is less pronounced than that for the disulfide bridges. Nevertheless, any QM refinement of protein structures without at least polarization functions on the S atoms is unlikely to yield acceptable R-factors. The findings also confirm our previous observations that cysteines are difficult to treat, and here, we have a likely explanation for this behavior.⁶ However, the advantage of using basis sets such as SV is, of course, the computational efficiency. One strategy with low computational cost and a practical level of accuracy

may be to use SVP on S-atoms only and SV for all other elements. This in combination with HF-D3-gCP is a possible practicable level of theory that can be tested in future QM refinement applications. Note that the gCP correction would need to be applied with the parametrization for SV and not SVP, as sulfur atoms were not included in the fit set used to determine the gCP parameters.

4.3. Results for the Water Hexamers. During the optimizations of the three isomers (*book*, *cage*, *prism*; see top row of Figure 8) of the water hexamer, we made an important

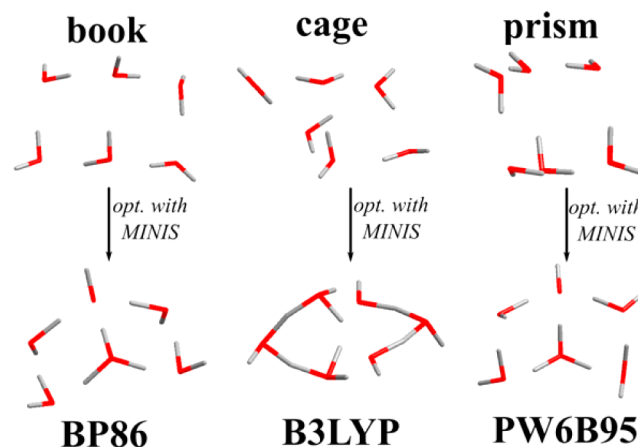


Figure 8. Top row: Experimental structures of the three water clusters. Bottom row: Example of autoionized water cluster geometries obtained with density functional methods and the MINIS basis set. The DFT-D3 and gCP corrections are employed in all cases, but these are not the source of the errors.

observation about using the minimal basis set MINIS. For all DFT methods other than B3LYP, all calculated hexamer structures were qualitatively inconsistent with experiment, as during the optimizations some water molecules formed hydronium and hydroxyl ions (see the lower row of Figure 8 for examples). This autoionization effect seems to depend on the amount of Fock exchange, as B3LYP and HF do not suffer from this problem. We could rule out the dispersion and BSSE corrections as possible error sources. Additional calculations with larger quadrature grids and the COSMO continuum solvation model⁶⁰ with a long-range dielectric constant of 4, a value that is often used to mimic protein environments, revealed the same behavior. Therefore, it is likely that basis-set incompleteness in combination with an inadequate description of exchange effects leads to this wrong description. When increasing the basis set size, the same was seen for some structures and levels of theory for the SV basis set. BP86 and PBE give autoionized structures for the *book* isomer, and BP86, B97-D, and PBE0 struggle with the description of the *prism* isomer.

For the water clusters, the averaged nearest O–O distances are analyzed herein (experimental values are shown in the lower rows of Table 3). Overall, the D3- and gCP corrections both have sizable effects on the averaged O–O distances (see Table S11, SI). The D3-correction leads to a shortening of the O–O distances, as discussed by Hujo and Grimme for the same systems,¹⁸ while gCP leads to a significant elongation (of up to 0.07 Å), meaning that BSSE effects are an important issue when using small basis sets. Overall D3- and gCP-corrected results are closest to the experimental values for most methods tested.

Table 3. Bond Lengths (Å) for HF-3c Compared to HF-D3-gCP/MINIS and Reference Values

	HF-3c	HF-D3-gCP/MINIS	ref ^a
C–O ^b	1.222	1.284	1.234
C–N ^b	1.379	1.409	1.350
C–C _α ^b	1.568	1.574	1.522
N–C _α ^b	1.456	1.488	1.453
S _γ –S _γ ^c	2.101	2.253	2.055
C _β –S _γ ^c	1.844	1.919	1.822
O–O (book) ^d	2.73	2.75	2.80
O–O (cage) ^d	2.77	2.78	2.85
O–O (prism) ^d	2.79	2.81	2.89
avg. error for O–O ^e	–0.09	–0.07	---

^aMP2/aug*-cc-pVTZ for P26 and CYS2; experimental values for the water hexamers. ^bAveraged bond lengths for the P26 set. ^cAveraged bond lengths for the CYS2 set. ^dAveraged O–O distances for the water hexamers. ^eAveraged error for O–O distances in water hexamers.

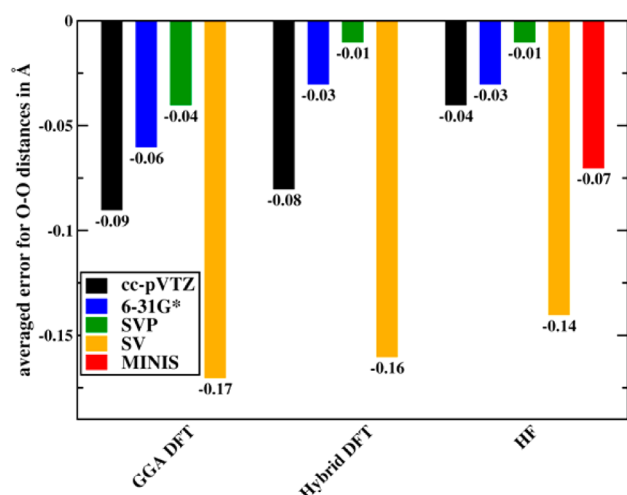
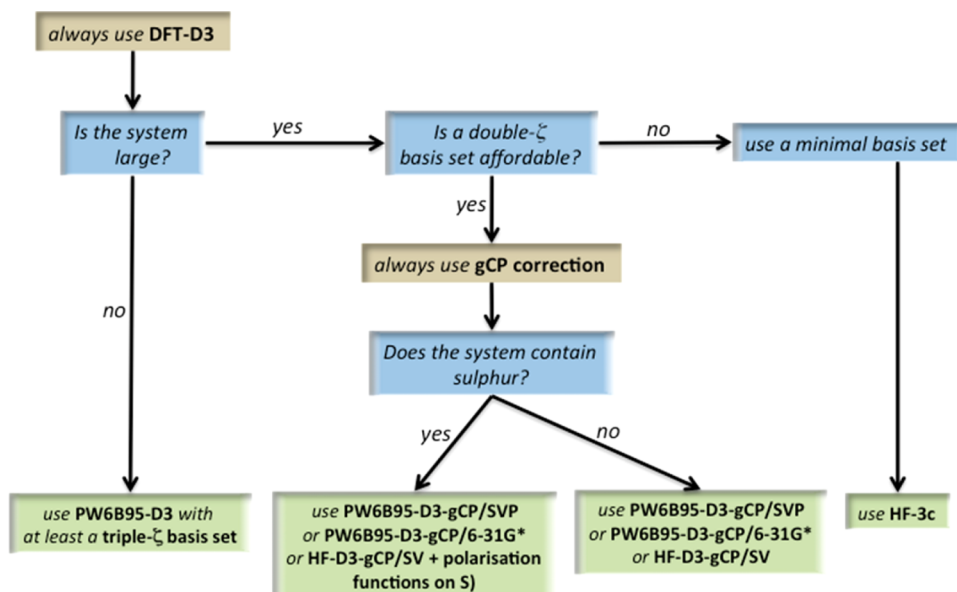
**Figure 9.** Averaged error for O–O distances in water hexamers for (meta-)GGA DFT, hybrid DFT, and HF. All methods were corrected with DFT-D3 and gCP and results for various basis sets are shown.

Figure 9 shows the averaged errors for the O–O distances for (meta-)GGAs, hybrid functionals, and HF for different basis sets. In all cases, the results were corrected for BSSE and dispersion effects. All levels of theory underestimate the O–O distance. The largest underestimation is seen for the SV basis set, while the smallest effects are observed for SVP and 6-31G*. The fact that cc-pVTZ underestimates the O–O distances more than the double- ζ basis sets is an indication that still some error-compensation effects play a role. HF-D3-gCP is for all basis sets the best option, although also hybrid functionals in combination with SVP show very similar errors. The results for HF-D3-gCP/MINIS lie in between those for SV and SVP.

4.4. Results for the HF-3c Method. We have identified the BSIE as a likely source for the elongated bond lengths in the examples discussed in this paper. Next, we test Grimme's new HF-3c, which combines the D3 and gCP corrections with a minimal basis set and a third empirical correction to overcome BSIE effects. It can also be seen as a complementing method to HF-D3-gCP/MINIS, and we therefore compare HF-3c with HF-D3-gCP/MINIS for our three test sets. As shown in the SI, the effects on RMSDs are not very big when comparing the two methods with each other. For P26, the averaged RMSD improves from 0.263 Å for HF-D3-gCP/MINIS to 0.223 Å for HF-3c. The averaged RMSD for CYS2 increases slightly from 0.177 Å for HF-D3-gCP/MINIS to 0.198 Å for HF-3c; the main cause here is conformer CYS2c, for which the RMSD increases from 0.236 Å to 0.300 Å, a value that is close to hybrid DFT for cc-pVTZ, to which the BSIE correction in HF-3c had been fitted.

The effect of HF-3c on bond lengths is significant and shown in Table 3 for all bond lengths discussed. In all cases, the bond lengths get shorter and resemble DFT results for double- and triple- ζ basis sets. HF-3c does not show the strong overbinding tendency of HF-D3/cc-pVTZ. The biggest effect is seen for the S–S and C–S bonds in the CYS2 test set. The averaged S–S bond length drops from 2.253 Å to 2.101 Å. C–S bond lengths are similarly described as GGA-DFT-D3/cc-pVTZ with 0.184 Å.

**Figure 10.** Conclusions and recommendations for the optimization of polypeptides.

The O–O distances in the water clusters are insignificantly shorter for HF-3c than for HF-D3-gCP/MINIS, because the third correction in HF-3c is designed for closer interatomic distances and does not have any significant effect on hydrogen bonds. The average error is -0.09 Å for HF-3c compared to -0.07 Å for HF-D3-gCP/MINIS.

5. SUMMARY AND RECOMMENDATIONS

For computational efficiency, the quantum chemical study of proteins is often carried out with Hartree–Fock (HF) or density functional theory (DFT) methods combined with small basis sets. However, these approaches face three major problems for the determination of structures to the quality required for say protein X-ray structure refinement applications. HF and current DFT approximations do not adequately describe London-dispersion effects, while small basis sets induce the basis-set superposition (BSSE) and basis-set incompleteness errors (BSIE); the focus of this work was assessing correction schemes for these problems. For HF and DFT, Grimme and co-workers established two corrections called DFT-D3 and gCP. These corrections have in common that they are time-efficient and easy to combine with standard efficient HF or DFT procedures. Sure and Grimme addressed the BSIE problem for HF with minimal basis sets, developing the HF-3c method, containing the D3-, and gCP corrections, and a third empirical correction to BSIE.

Our assessment of these methods utilized reoptimized gas-phase tripeptide structures of Hobza's P26 set, comprising 26 conformers of 5 tripeptides with aromatic side chains, a new set of three cysteine dimers connected by disulfide bridges, as well as water hexamer configurations. These test sets embody the most important features in protein crystal structures. One part of our analysis of these methods was based on root-mean-square deviations (RMSDs) from reference structures that assess intramolecular dispersion and hydrogen-bonding interactions. Additionally, all methods were also assessed based on calculated covalent bond lengths, as the successful treatment of proteins, such as quantum refinement, also depends on calculating these accurately.

In Figure 10 all of our findings are combined and used to make recommendations of practical, accurate computational strategies:

- (1) Regardless of the chosen basis set, dispersion corrections are crucial for both DFT and HF. We recommend Grimme's D3-correction in its latest version with Becke–Johnson damping. This correction makes HF a valuable and competitive alternative to dispersion-corrected DFT.
- (2) If the system size allows it, a basis set of at least triple- ζ quality, such as cc-pVTZ, should be chosen, as this reduces intramolecular BSSE effects. For a basis set of this quality, we favor the PW6B95-D3 method over other DFT approximations, but an alternative is also HF-D3 due to its low RMSDs.
- (3) If only a basis set of double- ζ quality can be used, it is crucial to correct for intramolecular BSSE and Grimme's new gCP correction is shown to be ideal. Although occasionally a method without this correction seems to yield better results, we demonstrate that this arises owing to unforeseeable error cancellation and that the DFT-D3-gCP and HF-D3-gCP approaches are more robust. Using the D3- and gCP-corrections minimizes error compensation to allow focusing on the quality of other aspects of

the computational methods. Depending on the type of basis set we conclude that PW6B95-D3-gCP is recommended when used with the 6-31G* and SVP basis sets, both double- ζ basis sets including polarization functions. If the system size prohibits usage of polarization functions, using the SV basis set with HF-D3-gCP is a valuable option, but in this case, polarization functions must be included on any sulfur atom.

- (4) If the system size does not allow using a double- ζ basis set, minimal basis sets provide the only option. Basis-set incompleteness effects are severe for minimal basis sets and are not accounted for when using the gCP correction. Indeed, for the MINIS basis set, we show that the DFT-D3-gCP and HF-D3-gCP methods yield unacceptably large bond lengths, making applications such as quantum refinement very difficult. Moreover, for most tested DFT methods, usage of MINIS leads to unphysical autoionization of water clusters. However, we show that the HF-3c method efficiently corrects for this problem to a large extent and provides a valuable new approach. We recommend extending this approach to include DFT methods.

The methods outlined in Figure 10 provide a wide range of efficient and accurate computational schemes that allow performing quantum chemical calculations on proteins and polypeptides for structure optimizations, molecular dynamics, and quantum refinement of protein X-ray structures.

■ ASSOCIATED CONTENT

Supporting Information

All Cartesian coordinates for the P26 and CYS2 test sets, all root-mean-square deviations for all tested methods, averaged covalent and hydrogen-bond lengths for P26 and CYS2, and all results for the water hexamers. This material is available free of charge via the Internet at <http://pubs.acs.org>.

■ AUTHOR INFORMATION

Corresponding Author

*E-mail: jeffrey.reimers@sydney.edu.au.

Notes

The authors declare no competing financial interest.

■ ACKNOWLEDGMENTS

Lars Goerigk is supported by a postdoctoral scholarship by the German Academy of Sciences "Leopoldina" under Grant No. LPDS 2011-11. This project was also supported by the Australian Research Council under Grant No. DP110102932. We are grateful for allocation of computer time from the NCI National Facility in Canberra, Australia, and from Intersect Australia Ltd. We thank Dr. Holger Kruse for technical support with the gCP code and Professor Stefan Grimme for providing us with a preprint of the HF-3c manuscript and a version of the related program.

■ REFERENCES

- (1) (a) Lahti, J. L.; Tang, G. W.; Capriotti, E.; Liu, T. Y.; Altman, R. B. *J. R. Soc. Interface* **2012**, *9*, 1409–1437. (b) Nugent, T.; Jones, D. T. *J. Struct. Biol.* **2012**, *179*, 327–337.
- (2) (a) Audie, J.; Swanson, J. *Chem. Biol. Drug Des.* **2013**, *81*, 50–60. (b) Du, Q. S.; Huang, R. B.; Chou, K. C. *Curr. Protein Pept. Sci.* **2008**, *9*, 248–259. (c) Concu, R.; Podda, G.; Ubeira, F. M.; Gonzalez-Diaz, H. *Curr. Pharm. Des.* **2010**, *16*, 2710–2723.

- (3) (a) Avila, L.; L., C. *Curr. Protein Pept. Sci.* **2011**, *12*, 221–234. (b) Falklöf, O.; Collyer, C. A.; Reimers, J. R. *Theor. Chem. Acc.* **2012**, *131*, 1076–1091. (c) Schmid, N.; Eichenberger, A.; Choutko, A.; Riniker, S.; Winger, M.; Mark, A.; van Gunsteren, W. *Eur. Biophys. J.* **2011**, *40*, 843–856. (d) Zhu, X.; Lopes, P. E. M.; MacKerell, A. D. *Wiley Interdiscip. Rev.: Comput. Mol. Sci.* **2012**, *2*, 167–185.
- (4) (a) Ryde, U.; Nilsson, K. J. *Am. Chem. Soc.* **2003**, *125*, 14232–14233. (b) Ryde, U.; Nilsson, K. J. *Mol. Struct.—Theochem* **2003**, *632*, 259–275. (c) Ryde, U. *Dalton Trans.* **2007**, 607–625. (d) Genheden, S.; Ryde, U. *J. Comput. Chem.* **2011**, *32*, 187–195. (e) Hsiao, Y. W.; Sanchez-Garcia, E.; Doerr, M.; Thiel, W. *J. Phys. Chem. B* **2010**, *114*, 15413–15423. (f) Yu, N.; Hayik, S. A.; Wang, B.; Liao, N.; Reynolds, C. H.; Merz, K. M., Jr. *J. Chem. Theory Comput.* **2006**, *2*, 1057–1069. (g) Li, X.; Hayik, S. A.; Merz, K. M. *J. Inorg. Biochem.* **2010**, *104*, 512–522. (h) Altun, A.; Shaik, S.; Thiel, W. *J. Comput. Chem.* **2006**, *27*, 1324–1337. (i) Hsiao, Y. W.; Thiel, W. *J. Phys. Chem. B* **2011**, *115*, 2097–2106. (j) Sanchez-Garcia, E.; Doerr, M.; Thiel, W. *J. Comput. Chem.* **2010**, *31*, 1603–1612. (k) Schoneboom, J. C.; Lin, H.; Reuter, N.; Thiel, W.; Cohen, S.; Ogliaro, F.; Shaik, S. *J. Am. Chem. Soc.* **2002**, *124*, 8142–8151. (l) Sun, Q.; Li, Z.; Lan, Z. G.; Pfisterer, C.; Doerr, M.; Fischer, S.; Smith, S. C.; Thiel, W. *Phys. Chem. Chem. Phys.* **2012**, *14*, 11413–11424.
- (5) Canfield, P.; Dahlbom, M. G.; Reimers, J. R.; Hush, N. S. *J. Chem. Phys.* **2006**, *124*, 024301.
- (6) Goerigk, L.; Falklöf, O.; Collyer, C. A.; Reimers, J. R.; Jeffrey, R. In *Quantum Simulations of Materials and Biological Systems*; Zeng, J.; Zhang, R.-Q.; Treutlein, H. R., Eds.; Springer: Dordrecht, 2012; pp 87–120.
- (7) Kulik, H. J.; Luehr, N.; Ufimtsev, I. S.; Martinez, T. J. *J. Phys. Chem. B* **2012**, *116*, 12501–12509.
- (8) Kohn, W.; Sham, L. J. *Phys. Rev.* **1965**, *140*, 1133–1138.
- (9) (a) White, C. A.; Johnson, B. G.; Gill, P. M. W.; Head-Gordon, M. *Chem. Phys. Lett.* **1996**, *253*, 268–278. (b) Lee, T. S.; Lewis, J. P.; Yang, W. *Comput. Mater. Sci.* **1998**, *12*, 259–277. (c) Wada, M.; Sakurai, M. *J. Comput. Chem.* **2005**, *26*, 160–168. (d) Fedorov, D. G.; Alexeev, Y.; Kitaura, K. *J. Phys. Chem. Lett.* **2010**, *2*, 282–288. (e) Fedorov, D. G.; Ishida, T.; Uebayasi, M.; Kitaura, K. *J. Phys. Chem. A* **2007**, *111*, 2722–2732. (f) Fedorov, D. G.; Kitaura, K. *J. Phys. Chem. A* **2007**, *111*, 6904–6914. (g) Nagata, T.; Brorsen, K.; Fedorov, D. G.; Kitaura, K.; Gordon, M. S. *J. Chem. Phys.* **2011**, *134*, 124115. (h) Nagata, T.; Fedorov, D. G.; Sawada, T.; Kitaura, K.; Gordon, M. S. *J. Chem. Phys.* **2011**, *134*, 034110. (i) Ohta, K.; Yoshioka, Y.; Morokuma, K.; Kitaura, K. *Chem. Phys. Lett.* **1983**, *101*, 12–17. (j) Gale, J. D. In *Computational Methods for Large Systems: Electronic Structure Approaches for Biotechnology and Nanotechnology*; Reimers, J. R., Ed.; Wiley: Hoboken, NJ, 2011; pp 45–74. (k) Mayhall, N. J.; Raghavachari, K. *J. Chem. Theory Comput.* **2010**, *7*, 1336–1343. (l) He, X.; Merz, K. M. *J. Chem. Theory Comput.* **2010**, *6*, 405–411. (m) Kussmann, J.; Beer, M.; Ochsenfeld, C. *Wiley Interdiscip. Rev.: Comput. Mol. Sci.* **2013**, DOI: 10.1002/wcms.1138. (n) Pruitt, S. R.; Steinmann, C.; Jensen, J. H.; Gordon, M. S. *J. Chem. Theory Comput.* **2013**, *9*, 2235–2249.
- (10) (a) Kristyán, S.; Pulay, P. *Chem. Phys. Lett.* **1994**, *229*, 175–180. (b) Hobza, P.; Šponer, J.; Reschel, T. *J. Comput. Chem.* **1995**, *16*, 1315–1325. (c) Šponer, J.; Leszczynski, J.; Hobza, P. *J. Comput. Chem.* **1996**, *17*, 841–850.
- (11) (a) Kolar, M.; Kubar, T.; Hobza, P. *J. Phys. Chem. B* **2011**, *115*, 8038–8046. (b) Tkatchenko, A.; Rossi, M.; Blum, V.; Ireta, J.; Scheffler, M. *Phys. Rev. Lett.* **2011**, *106*, 118102.
- (12) (a) Antony, J.; Grimme, S. *Phys. Chem. Chem. Phys.* **2006**, *8*, 5287–5293. (b) Antony, J.; Grimme, S. *J. Comput. Chem.* **2012**, *33*, 1730–1739. (c) Antony, J.; Grimme, S.; Liakos, D. G.; Neese, F. *J. Phys. Chem. A* **2011**, *115*, 11210–11220. (d) Grimme, S. *J. Comput. Chem.* **2006**, *27*, 1787–1799. (e) Grimme, S. *J. Comput. Chem.* **2004**, *25*, 1463–1473. (f) Grimme, S.; Antony, J.; Schwabe, T.; Muck-Lichtenfeld, C. *Org. Biomol. Chem.* **2007**, *5*, 741–758. (g) Schwabe, T.; Grimme, S. *Phys. Chem. Chem. Phys.* **2007**, *9*, 3397–3406. (h) Waller, M. P.; Kruse, H.; Muck-Lichtenfeld, C.; Grimme, S. *Chem. Soc. Rev.* **2012**, *41*, 3119–3128.
- (13) Grimme, S. *Wiley Interdiscip. Rev.: Comput. Mol. Sci.* **2011**, *1*, 211–228.
- (14) (a) Grimme, S.; Antony, J.; Ehrlich, S.; Krieg, H. *J. Chem. Phys.* **2010**, *132*, 154104. (b) Grimme, S.; Ehrlich, S.; Goerigk, L. *J. Comput. Chem.* **2011**, *32*, 1456–1465.
- (15) Goerigk, L.; Kruse, H.; Grimme, S. *ChemPhysChem* **2011**, *12*, 3421–3433.
- (16) Goerigk, L.; Grimme, S. *Phys. Chem. Chem. Phys.* **2011**, *13*, 6670–6688.
- (17) Grimme, S.; Schreiner, P. R. *Angew. Chem., Int. Ed.* **2011**, *50*, 12639–12642.
- (18) Hujo, W.; Grimme, S. *J. Chem. Theory Comput.* **2012**, *9*, 308–315.
- (19) Roskop, L.; Fedorov, D. G.; Gordon, M. S. *Mol. Phys.* **2013**, DOI: 10.1080/00268976.2013.780102.
- (20) (a) Kestner, N. R. *J. Chem. Phys.* **1968**, *48*, 252. (b) Jansen, H. B.; Ros, P. *Chem. Phys. Lett.* **1969**, *3*, 140–143. (c) Liu, B.; McLean, A. D. *J. Chem. Phys.* **1973**, *59*, 4557–4558. (d) van Duijneveldt, F. B.; van Duijneveldt-van de Rijdt, J. G. C. M.; van Lenthe, J. H. *Chem. Rev.* **1994**, *94*, 1873–1885.
- (21) Kruse, H.; Grimme, S. *J. Chem. Phys.* **2012**, *136*, 154101.
- (22) Boys, S. F.; Bernardi, F. *Mol. Phys.* **1970**, *19*, 553–566.
- (23) (a) Mayer, I.; Turi, L. *J. Mol. Struct.—Theochem* **1991**, *73*, 43–65. (b) Cook, D. B.; Sordo, J. A.; Sordo, T. L. *Int. J. Quantum Chem.* **1993**, *48*, 375–384. (c) Gutowski, M.; Chalasinski, G. *J. Chem. Phys.* **1993**, *98*, 5540–5554. (d) Wiczorek, R.; Haskamp, L.; Dannenberg, J. J. *J. Phys. Chem. A* **2004**, *108*, 6713–6723.
- (24) (a) Mayer, I. *Int. J. Quantum Chem.* **1983**, *23*, 341–363. (b) Asturiol, D.; Duran, M.; Salvador, P. *J. Chem. Phys.* **2008**, *128*, 144108. (c) Balabin, R. M. *J. Chem. Phys.* **2010**, *132*, 231101. (d) Jensen, F. *J. Chem. Theory Comput.* **2010**, *6*, 100–106. (e) Deng, J.; Gilbert, A. T. B.; Gill, P. M. W. *J. Chem. Phys.* **2011**, *135*, 081105.
- (25) (a) Holroyd, L. F.; van Mourik, T. *Chem. Phys. Lett.* **2007**, *442*, 42–46. (b) van Mourik, T.; Karamertzanis, P. G.; Price, S. L. *J. Phys. Chem. A* **2006**, *110*, 8–12. (c) Valdes, H.; Klusak, V.; Pitonak, M.; Exner, O.; Stry, I.; Hobza, P.; Rulisek, L. *J. Comput. Chem.* **2008**, *29*, 861–870.
- (26) Kruse, H.; Goerigk, L.; Grimme, S. *J. Org. Chem.* **2012**, *77*, 10824–10834.
- (27) Sure, R.; Grimme, S. *J. Comput. Chem.* **2013**, DOI: 10.1002/jcc.23317.
- (28) (a) Moreno, J. R. A.; Moreno, M. D. Q.; Urena, F. P.; Gonzalez, J. J. *Tetrahedron: Asymmetry* **2012**, *23*, 1084–1092. (b) Bohórquez, H. J.; Cárdenas, C.; Matta, C. F.; Boyd, R. J.; Patarroyo, M. E. In *Quantum Biochemistry*; Matta, C. F., Ed.; Wiley-VCH Verlag GmbH & Co. KGaA: Weinheim, Germany, 2010; pp 403–421. (c) Wilke, J. J.; Lind, M. C.; Schaefer, H. F.; Csaszar, A. G.; Allen, W. D. *J. Chem. Theory Comput.* **2009**, *5*, 1511–1523.
- (29) (a) Cerny, J.; Jurecka, P.; Hobza, P.; Valdes, H. *J. Phys. Chem. A* **2007**, *111*, 1146–1154. (b) Gloaguen, E.; Valdes, H.; Pagliarulo, F.; Pollet, R.; Tardivel, B.; Hobza, P.; Piuze, F.; Mons, M. *J. Phys. Chem. A* **2010**, *114*, 2973–2982. (c) Reha, D.; Valdes, H.; Vondrasek, J.; Hobza, P.; Abu-Riziq, A.; Crews, B.; de Vries, M. S. *Chem.—Eur. J.* **2005**, *11*, 6803–6817. (d) Valdes, H.; Pluhackova, K.; Hobza, P. *J. Chem. Theory Comput.* **2009**, *5*, 2248–2256. (e) Valdes, H.; Reha, D.; Hobza, P. *J. Phys. Chem. B* **2006**, *110*, 6385–6396. (f) Valdes, H.; Spiwok, V.; Rezac, J.; Reha, D.; Abo-Riziq, A. G.; de Vries, M. S.; Hobza, P. *Chem.—Eur. J.* **2008**, *14*, 4886–4898. (g) Toroz, D.; van Mourik, T. *Mol. Phys.* **2006**, *104*, 559–570.
- (30) Goerigk, L.; Karton, A.; Martin, J. M. L.; Radom, L. *Phys. Chem. Chem. Phys.* **2013**, *15*, 7028–7031.
- (31) Valdes, H.; Pluhackova, K.; Pitonak, M.; Rezac, J.; Hobza, P. *Phys. Chem. Chem. Phys.* **2008**, *10*, 2747–2757.
- (32) Perez, C.; Muckle, M. T.; Zaleski, D. P.; Seifert, N. A.; Temelso, B.; Shields, G. C.; Kisiel, Z.; Pate, B. H. *Science* **2012**, *336*, 897–901.
- (33) Kendall, R. A.; Dunning, T. H.; Harrison, R. J. *J. Chem. Phys.* **1992**, *96*, 6796–6806.
- (34) (a) Halkier, A.; Koch, H.; Jorgensen, P.; Christiansen, O.; Beck Nielsen, I. M.; Helgaker, T. *Theor. Chem. Acc.* **1997**, *97*, 150–157.

- (b) Jurecka, P.; Cerny, J.; Hobza, P.; Salahub, D. *J. Comput. Chem.* **2007**, *28*, 555–569.
- (35) (a) Goerigk, L.; Grimme, S. *J. Chem. Theory Comput.* **2010**, *6*, 107–126. (b) Goerigk, L.; Grimme, S. *J. Chem. Theory Comput.* **2011**, *7*, 291–309.
- (36) Grimme, S. *J. Chem. Phys.* **2003**, *118*, 9095–9102.
- (37) (a) Grimme, S. *J. Chem. Phys.* **2006**, *124*, 034108. (b) Neese, F.; Schwabe, T.; Grimme, S. *J. Chem. Phys.* **2007**, *126*, 124115.
- (38) Rupp, B. *Biomolecular Crystallography—Principles, Practice, and Application to Structural Biology*; Garland Science: New York, 2010.
- (39) (a) Gustus, E. L. *J. Org. Chem.* **1967**, *32*, 3425–3430. (b) Takagi, T.; Okano, R.; Miyazawa, T. *Biochim. Biophys. Acta* **1973**, *310*, 11–19.
- (c) Hill, R. R.; Ghadimi, M. *J. Soc. Dyers Colour* **1996**, *112*, 148–152.
- (40) (a) TURBOMOLE V6.4 2012, a development of University of Karlsruhe and Forschungszentrum Karlsruhe GmbH, 1989–2007, TURBOMOLE GmbH, since 2007; available from <http://www.turbomole.com> (accessed May 23, 2013); (b) Ahlrichs, R.; Bar, M.; Haser, M.; Horn, H.; Kolmel, C. *Chem. Phys. Lett.* **1989**, *162*, 165–169.
- (41) Weigend, F.; Haser, M. *Theor. Chem. Acc.* **1997**, *97*, 331.
- (42) Becke, A. D. *Phys. Rev. A* **1988**, *38*, 3098–3100.
- (43) Lee, C.; Yang, W.; Parr, R. G. *Phys. Rev. B* **1988**, *37*, 785–789.
- (44) Perdew, J. P.; Wang, Y. *Phys. Rev. B* **1986**, *33*, 8800–8802.
- (45) Perdew, J. P.; Burke, K.; Ernzerhof, M. *Phys. Rev. Lett.* **1996**, *77*, 3865–3868.
- (46) Tao, J. M.; Perdew, J. P.; Staroverov, V. N.; Scuseria, G. E. *Phys. Rev. Lett.* **2003**, *91*, 146401.
- (47) (a) Becke, A. D. *J. Chem. Phys.* **1993**, *98*, 5648–5652. (b) Stephens, P. J.; Devlin, F. J.; Chabalowski, C. F.; Frisch, M. J. *J. Phys. Chem.* **1994**, *98*, 11623–11627.
- (48) (a) Ernzerhof, M.; Scuseria, G. E. *J. Chem. Phys.* **1999**, *110*, 5029–5036. (b) Adamo, C.; Barone, V. *J. Chem. Phys.* **1999**, *110*, 6158–6170.
- (49) Zhao, Y.; Truhlar, D. G. *J. Phys. Chem. A* **2005**, *109*, 5656–5667.
- (50) Becke, A. D. *J. Chem. Phys.* **1993**, *98*, 1372–1377.
- (51) Hehre, W. J.; Ditchfield, R.; Pople, J. A. *J. Chem. Phys.* **1972**, *56*, 2257–2261.
- (52) Horn, H.; Ahlrichs, R. *J. Chem. Phys.* **1992**, *97*, 2571–2577.
- (53) Tatewaki, H.; Huzinaga, S. *J. Comput. Chem.* **1980**, *1*, 205–228.
- (54) EMSL basis-set exchange, <https://bse.pnl.gov/bse/portal> (accessed Apr. 18, 2013).
- (55) Eichkorn, K.; Treutler, O.; Ohm, H.; Haser, M.; Ahlrichs, R. *Chem. Phys. Lett.* **1995**, *240*, 283–289.
- (56) Eichkorn, K.; Weigend, F.; Treutler, O.; Ahlrichs, R. *Theor. Chem. Acc.* **1997**, *97*, 119–124.
- (57) Website of the Grimme group, <http://www.thch.uni-bonn.de/tc/index.php?section=downloads&lang=english> (accessed May 23, 2013).
- (58) Jensen, F. *Introduction to Computational Chemistry*, 2nd ed.; John Wiley & Sons: New York, 2007.
- (59) Petersen, M. T. N.; Jonson, P. H.; Petersen, S. B. *Protein Eng.* **1999**, *12*, 535–548.
- (60) Klamt, A.; Schuurmann, G. *J. Chem. Soc., Perkin Trans. 2* **1993**, 799–805.